Using Probability Maps for Multi–organ Automatic Segmentation

Ranveer Joyseeree[1,2], Óscar Jiménez del Toro[1], and Henning Müller[1,3]

[1] University of Applied Sciences Western Switzerland (HES–SO), Sierre, Switzerland
[2] Eidgenössische Technische Hochschule (ETH), Zürich, Switzerland
[3] Medical Informatics, University Hospitals & University of Geneva, Switzerland

Abstract. Organ segmentation is a vital task in diagnostic medicine. The ability to perform it automatically can save clinicians time and labor. In this paper, a method to achieve automatic segmentation of organs in three–dimensional (3D), non–annotated, full–body magnetic resonance (MR), and computed tomography (CT) volumes is proposed.
According to the method, training volumes are registered to a chosen reference volume and the registration transform obtained is used to create an overlap volume for each annotated organ in the dataset. A 3D probability map, and its centroid, is derived from that. Afterwards, the reference volume is affinely mapped onto any non–annotated volume and the obtained mapping is applied to the centroid and the organ probability maps.
Region–growing segmentation on the non–annotated volume may then be started using the warped centroid as the seed point and the warped probability map as an aid to the stopping criterion.

Keywords: medical image processing, region–growing, segmentation

1 Introduction

Clinicians have come to rely very heavily on imaging for diagnosis and pre–operative surgical planning. Segmentation is often an essential step in the analysis of patient data. Automatic segmentation can greatly reduce the burden on clinicians who are called upon for manual delineation of organs in full–body scans or other images. They can, thus, save time which they could invest in other aspects of their work in order to provide better care to patients. To achieve this goal, a method to automatically segment the contents of full–body MR/CT scans using probability maps built from training images is proposed in this paper.

Moreover, medical information is being produced and collected at a massive rate and there is a clear need for its efficient processing and storage. This is particularly important in order to effectively exploit the information contained in images gathered for past clinical cases in order to improve diagnosis and surgical planning outcomes. Automating the processing and efficient storage of the huge quantities of data being collected is thus becoming vital. The proposed

automatic segmentation technique would help greatly with that. In addition, it will eventually allow for automatic organ classification and, subequently, effective archiving and storage for later retrieval.

Furthermore, this study is well aligned with the FP7 VISual Concept Extraction challenge in RAdioLogy (VISCERAL) [5] benchmark[4] which involves achieving automatic segmentation of anatomical structures in non–annotated full–body MR/ CT volumes. The project also involves the segmentation of a 'surprise' organ. Only training data and no a–priori knowledge can be used for that purpose. A segmentation method that uses the proposed method of using probability maps built from training images would be perfectly suited to achieve it.

2 Methods

A full–body MR or CT volume, labelled as X, is chosen from the database of training acquisitions, Y_1 to Y_N (where N is the size of the database), provided for VISCERAL. Each acquisition has been examined by expert radiologists who have annotated up to 20 different organs and saved each annotation, labelled A(Y_n,organ) (where n is the identifier of a particular volume in the database), as a separate volume.

Care is taken such that X is not an outlier in terms of body shape and size. This ensures that the error introduced by affine registration, which will be used in the next step, is kept to a minimum. Figure 1 illustrates the choice of X for this paper and includes an illustrative annotation, $A(X$,liver) in blue.

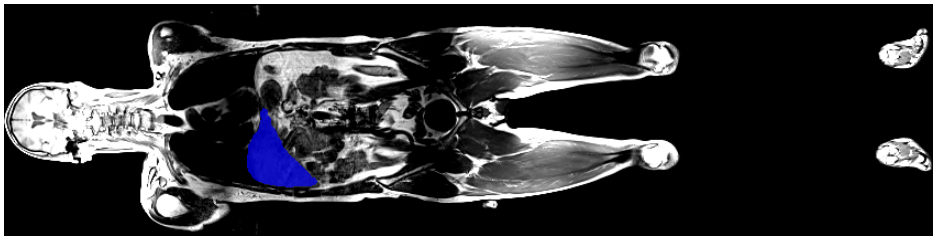

Fig. 1: A full–body MR volume is chosen as X. For illustrative purposes, X is superimposed with the liver annotation: $A(X$,liver)

2.1 Registration

A training volume, labelled as Y_1, is then registered with X. Y_1 is chosen as the moving volume and X is the fixed volume. An affine transformation [1] is applied during the registration process as it offers a good compromise between

[4] VISCERAL benchmark: http://www.visceral.eu/benchmark-1/, 2012. [Online; accessed 31–July–2013].

computation speed and accuracy. The cost metric used is mutual information (MI) [2] as two modalities — MR and CT — may need to be registered together.

To speed up the computation of MI, the implementation by Mattes et al. [6, 7] is utilized. To minimize the interpolation errors that necessarily occur during registration while keeping computation time low, B–Spline interpolation [9, 10, 8] is carried out. After the successful completion of registration, the linear transform T that maps Y_1 onto X is obtained.

Next, one organ of interest, Z, is picked. The annotation volume, A(Y_1,Z), is then converted into a binary volume before being transformed using T, giving $A^T(Y_1, Z)$. The latter is resampled such that it has the exact volume and voxel dimensions as $A(X, Z)$, which itself has the same mensurations as X.

2.2 Creation of a Probability Distribution Volume

To create a probability distribution volume, the above registration step is carried out for all N available VISCERAL volumes. For each training volume Y_n, a different transformation T and a different warped annotated volume $A^T(Y_n, Z)$ are obtained.

Since $A^T(Y_n, Z)$ for all n have the same volume and voxel sizes as $A(X, Z)$, they may be combined together voxel–wise and then normalized according to equation (1) to obtain the probability distribution volume for organ Z: PD_Z.

Please note that $A(X, Z)$ is present in (1) as $A^T(X, Z)$ since X is a member of the set $(Y_1, Y_2, ..., Y_N)$ and $A(X, Z) = A^T(X, Z)$.

$$PD_Z = \frac{1}{N} \sum_{n=1}^{N} A^T(Y_n, Z) \tag{1}$$

2.3 Generation of a Seed Point

The centroid of PD_Z, represented in row vector form as $\begin{bmatrix} x_c & y_c & z_c \end{bmatrix}$, corresponds to the weighted average location of a point that lies within PD_Z. For an MxNxP volume, it can be found using equation (2), where $V(x, y, z)$ is the voxel value at coordinates (x, y, z), which is represented as $\begin{bmatrix} x & y & z \end{bmatrix}$ in vector form. For a volume, B, on which the seed point for segmentation has to be found, affine registration between X and B is carried out. This time, X is used as the moving image while B is the fixed volume. The obtained transformation is applied to the volume containing the centroid found above. The location of the warped centroid may now be used as a seed point for segmentation on volume B.

$$\begin{bmatrix} x_c & y_c & z_c \end{bmatrix} = \frac{\sum_{x=1}^{M} \sum_{y=1}^{N} \sum_{z=1}^{P} V(x, y, z) * \begin{bmatrix} x & y & z \end{bmatrix}}{\sum_{x=1}^{M} \sum_{y=1}^{N} \sum_{z=1}^{P} V(x, y, z)} \tag{2}$$

2.4 Region–growing Algorithm for Segmentation

Current region–growing algorithms only use the properties of voxels in the neighbourhood of the seed point in order to determine if a certain voxel belongs to

the organ being segmented or not. In this paper, a method to supplement the conventional voxel–based approach with information contained in the warped probability map is proposed. At the time of writing, investigations to find such a hybrid measure to discriminate between voxels are on–going. Current work is focused on the weeding out of regions of lower probability value from the probability maps in order to determine the effect of doing that on the overlap between the new probability maps and the reference organ annotation.

3 Preliminary Results

For a series of up to 9 MR/CT volumes corresponding to four types of organ annotations: the left lung, the liver, the left kidney, and the urinary bladder, the respective probability distribution volumes are computed. Figure 2a shows the one for the liver, PD_{liver}, in coronal view . The darkest red region indicates a probability of one for a voxel to lie inside the liver and the darkest blue region indicates a probability of zero. The visualisation was generated using 3D Slicer[5] [4].

Figure 2b illustrates the centroid of PD_{liver} as a very dark red point near the centre of the probability distribution. When the same procedure is applied to the right lung, right kidney and the urinary bladder, Figure3–6 are obtained respectively. It may be observed that the seed points are located well within the target organs, implying that the automatic computation of organ seed points yields satisfactory results.

Currently, methods to improve the overlap between the probability maps and the reference annotations are being investigated. It is quantified using Dice's coefficient [3]. Preliminary results of the investigation are displayed in Figure 7. It is clearly shown in it that the Dice coefficient and, therefore, the overlap between the maps and the reference annotation may be improved by neglecting lower probabilities in the probability maps up to a certain point. This has interesting implications for the use of probability maps as a control for region–growing in segmentation algorithms. It is expected that further investigation into this property of probability maps will be useful in devising an effective stopping criterion.

[5] 3D Slicer: http://www.slicer.org, 2013. [Online; accessed 31–July–2013].

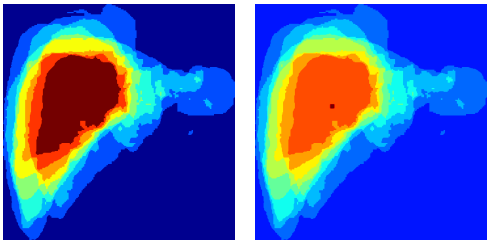

(a) (b)

Fig. 2: (a) Probability distribution volume of the liver (coronal view). The darkest red region indicates a probability of 1 for a voxel to lie on the liver and the dark blue region indicates a probability of 0; (b) The centroid of the liver is the darkest point in the probability distribution volume.

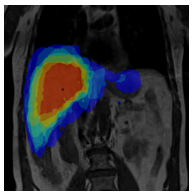

Fig. 3: Dark red seed point on X and PD_{liver}

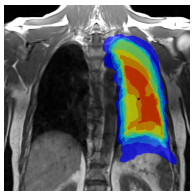

Fig. 4: Seed point on X and PD_{left_lung}

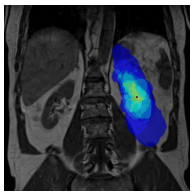

Fig. 5: Seed point on X and PD_{left_kidney}

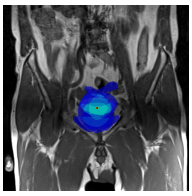

Fig. 6: Seed point on X and $PD_{urinary\_bladder}$

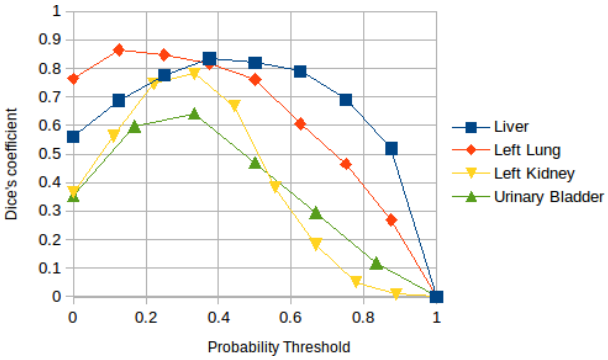

Fig. 7: Evolution in the Dice coefficient as the probability threshold is increased. Overlap may be improved by neglecting regions of lower probability up to a certain threshold.

4 Conclusions

This article proposes a very generic, simple, scalable, and easy–to–implement approach to achieve the automatic segmentation of any organ based on annotated 3D training data. Initial results indicate that it is effective in finding satisfactory seed points automatically. Once the measure to discriminate between voxels during region–growing is devised using voxel properties and 3D probability maps, it is expected that fully automatic segmentation will be convincingly achieved.

However, some limitations to the approach are foreseen. Due to the significantly large mismatch between the body–shape, the technique will perform poorly when applied to MR/CT scans of children or people with extreme body shapes such as obese or extremely long persons. Nevertheless, the technique described in this paper is expected to perform well in all other cases. It is also expected that it will achieve the goals of the VISCERAL benchmark and eventually play a significant role in the improvement in the way the ever–increasing mass of collected medical data is processed and stored.

References

1. Berger, M.: Geometry. I. Universitext. Springer-Verlag, Berlin (1987)
2. Cover, T.M., Thomas, J.A.: Entropy, relative entropy and mutual information. Elements of Information Theory pp. 12–49 (1991)
3. Dice, L.R.: Measures of the amount of ecologic association between species. Ecology 26(3), 297–302 (1945)
4. Fedorov, A., Beichel, R., Kalpathy-Cramer, J., Finet, J., Fillion-Robin, J.C., Pujol, S., Bauer, C., Jennings, D., Fennessy, F., Sonka, M., et al.: 3d slicer as an image computing platform for the quantitative imaging network. Magnetic Resonance Imaging (2012)
5. Langs, G., Müller, H., Menze, B.H., Hanbury, A.: Visceral: Towards large data in medical imaging — challenges and directions. In: Medical Content–based Retrieval for Clinical Decision Support. MCBR–CDS 2012 (Oct 2012)
6. Mattes, D., Haynor, D.R., Vesselle, H., Lewellen, T.K., Eubank, W.: Nonrigid multimodality image registration. Medical Imaging 4322(1), 1609–1620 (2001)
7. Mattes, D., Haynor, D.R., Vesselle, H., Lewellen, T.K., Eubank, W.: Pet-ct image registration in the chest using free-form deformations. IEEE Transactions on Medical Imaging 22(1), 120–128 (2003)
8. Unser, M.: Splines: A perfect fit for signal and image processing. IEEE Signal Processing Magazine 16(6), 22–38 (1999)
9. Unser, M., Aldroubi, A., Eden, M.: B-spline signal processing. i. theory. IEEE Transactions on Signal Processing 41(2), 821–833 (1993)
10. Unser, M., Aldroubi, A., Eden, M.: B-spline signal processing. ii. efficiency design and applications. IEEE Transactions on Signal Processing 41(2), 834–848 (1993)